VTRC
Virginia Transportation Research Council

We Bring Innovation to Transportation

Time-Lapse Infrared Thermography Applied to Concrete Bridge Deck Inspection Surveys

http://www.virginiadot.org/vtrc/main/online_reports/pdf/20-r22.pdf

STEVEN B. CHASE, Ph.D.
Research Professor

CHAD M. ANDERSON, EIT
Ph.D. Candidate

Department of Civil and Environmental Engineering
University of Virginia

Final Report VTRC 20-R22

VIRGINIA TRANSPORTATION RESEARCH COUNCIL
530 Edgemont Road, Charlottesville, VA 22903-2454
vtrc.virginiadot.org

Standard Title Page - Report on Federally Funded Project

1. Report No.: FHWA/VTRC 20-R22	2. Government Accession No.:	3. Recipient's Catalog No.:
4. Title and Subtitle: Time-Lapse Infrared Thermography Applied to Concrete Bridge Deck Inspection Surveys		5. Report Date: March 2020 6. Performing Organization Code:
7. Author(s): Steven B. Chase, Ph.D., and Chad M. Anderson, EIT		8. Performing Organization Report No.: VTRC 20-R22
9. Performing Organization and Address: Virginia Transportation Research Council 530 Edgemont Road Charlottesville, VA 22903		10. Work Unit No. (TRAIS): 11. Contract or Grant No.: 106624
12. Sponsoring Agencies' Name and Address: Virginia Department of Transportation 1401 E. Broad Street Richmond, VA 23219 Federal Highway Administration 400 North 8th Street, Room 750 Richmond, VA 23219-4825		13. Type of Report and Period Covered: Final Contract 14. Sponsoring Agency Code:
15. Supplementary Notes: This is an SPR-B report		

16. Abstract:

The Federal Highway Administration mandates that all [bridge] structures in its inventory are to be inspected every two years. Consequently, deck surveys are conducted to identify unseen damage within them. A significant number of bridges in Virginia have concrete decks with an overlay. Methods commonly deployed on these decks, are limited in the quantitative results they can provide. To overcome these limitations, an improved method of applying infrared thermography using time-lapse technology is introduced. Following a simulated parametric study, a time-lapse infrared thermography data collection system was acquired along with a basic program to analyze the data qualitatively.

A novel physics-based program was also developed to analyze the data quantitatively. The system is ready to be deployed on most bridges, offering a full-field non-contact survey of the entire deck with minimal impact to traffic flow. However, it is recommended that the quantitative program undergo additional testing prior to production level deployment.

17 Key Words: Nondestructive evaluation, instrumentation, infrared thermography, time lapse infrared thermography, deck inspection, delamination, debondment	18. Distribution Statement: No restrictions. This document is available to the public through NTIS, Springfield, VA 22161.		
19. Security Classif. (of this report): Unclassified	20. Security Classif. (of this page): Unclassified	21. No. of Pages: 31	22. Price:

Form DOT F 1700.7 (8-72) Reproduction of completed page authorized

FINAL REPORT

TIME-LAPSE INFRARED THERMOGRAPHY APPLIED TO CONCRETE BRIDGE DECK INSPECTION SURVEYS

Steven B. Chase, Ph.D.
Research Professor

Chad M. Anderson, EIT
Ph.D. Candidate

Department of Civil and Environmental Engineering
University of Virginia

VTRC Project Manager
Soundar Balakumaran, Ph.D., P.E., Virginia Transportation Research Council

In Cooperation with the U.S. Department of Transportation
Federal Highway Administration

Virginia Transportation Research Council
(A partnership of the Virginia Department of Transportation
and the University of Virginia since 1948)

Charlottesville, Virginia

March 2020
VTRC 20-R22

DISCLAIMER

The project that is the subject of this report was done under contract for the Virginia Department of Transportation, Virginia Transportation Research Council. The contents of this report reflect the views of the authors, who are responsible for the facts and the accuracy of the data presented herein. The contents do not necessarily reflect the official views or policies of the Virginia Department of Transportation, the Commonwealth Transportation Board, or the Federal Highway Administration. This report does not constitute a standard, specification, or regulation. Any inclusion of manufacturer names, trade names, or trademarks is for identification purposes only and is not to be considered an endorsement.

Each contract report is peer reviewed and accepted for publication by staff of the Virginia Transportation Research Council with expertise in related technical areas. Final editing and proofreading of the report are performed by the contractor.

ABSTRACT

The Federal Highway Administration mandates that all bridges should be inspected every two years. Consequently, deck surveys are conducted to identify unseen damage within them. A significant number of bridges in Virginia have concrete decks with an overlay. Methods commonly deployed on these decks are limited in the quantitative results they can provide. To overcome these limitations, an improved method of applying infrared thermography using time-lapse technology is introduced. Following a simulated parametric study, a time-lapse infrared thermography data collection system was acquired along with a basic program to analyze the data qualitatively. This qualitative analysis provides visual detection of surface thermal anomalies typically associated with concrete bridge deck delaminations and/or overlay debondment.

A novel physics-based program was also developed to analyze the data quantitatively. The quantitative analysis distinguishes between a delamination or overlay debondment and provides depth to defect results. The system is ready to be deployed on most bridges, offering a full-field non-contact survey of the entire deck with minimal impact to traffic flow. It is recommended that the quantitative program undergo additional testing prior to production level deployment.

FINAL REPORT

TIME-LAPSE INFRARED THERMOGRAPHY APPLIED TO CONCRETE BRIDGE DECK INSPECTION SURVEYS

Steven B. Chase, Ph.D.
Research Professor

Chad M. Anderson, EIT
Ph.D. Candidate

Department of Civil and Environmental Engineering
University of Virginia

INTRODUCTION

Background

Excluding culverts, most of the bridges in Virginia have cast in place reinforced concrete decks. About half of these decks have an overlay of some type, as shown in Table 1. The data presented in Table 1 was acquired from the National Bridge Inventory (NBI). The NBI is made available by the U.S. Department of Transportation on the Federal Highway Administration (FHWA) website (www.fhwa.dot.gov). The presence of an overlay makes the visual detection of defects in the underlying structural concrete deck difficult because common bridge deck evaluation tools such as chain-drag and impact echo do not work on overlaid bridge decks. It is also the case, that many decks without an overlay have extra concrete on the surface, with increased depth to the reinforcing steel. This also reduces the reliability of the common nondestructive evaluation (NDE) methods. The Virginia Department of Transportation (VDOT) expressed interest in investigating other NDE methods for application to overlaid bridge decks.

Table 1. RC Bridge Decks in Virginia

Deck Surface	Count	Area (sq. ft.)
Bare Deck	4,723	5,217,385
AC Wearing Surface	2,607	458,374
Latex	1,036	1,220,642
Epoxy	970	1,067,892
Other	89	28,678

RC: Reinforced Concrete, AC: Asphalt Concrete

The two most likely methods are ground penetrating radar (GPR) and infrared thermography. VDOT has had experience with both of these methods. The current state of the art of both of these NDE methods is briefly discussed to help explain why this project was needed.

Ground Penetrating Radar

GPR can provide data on the presence or absence of discontinuities and abrupt differences in the dielectric properties of a bridge deck. The presence of rebar, voids, large delaminations, disbondments and other features which present abrupt changes in the dielectric properties of the slab will result in characteristic echoes in the pulse response display of a typical GPR system. For high speed, non-contact GPR inspections, the antenna is usually vehicle mounted and driven over a deck with the ambient traffic. This type of application provides strips of data corresponding to the path of the antennae as it passes over the bridge deck. Post processing of the data is performed visually or with special computer software to identify specific characteristic patterns in the data associated with common defects. The presence of an overlay can have a significant impact on GPR data. First, the overlay can be several inches thick and adds dielectric losses to the transmitted and return paths as well as additional time delays to the signal. If there is a significant reflective feature in the deck, then it might not allow sufficient radar energy to penetrate below that level.

Conventional Infrared Thermography

Conventional infrared thermography (IRT) has also been used to inspect bridge decks and can also provide data about subsurface delaminations. Any subsurface feature which affects the flow of heat through the bridge deck might result in differences in the surface temperature of the slab, relative to a bridge deck without such features. Traditionally, the source of heat is solar radiation. As the sun irradiates the bridge deck surface, heat transfer takes place, which causes the surface of the bridge deck to become warmer than the interior of the deck. Heat will then flow from the surface of the deck to the interior by means of conduction. If there is a feature that retards the conduction of heat, such as a delamination, then the surface temperature at that location will become warmer, relative to a location where such a feature is absent. However, this process is transient and influenced by a number of factors. The solar radiation varies throughout the day and season. It is also subject to additional variations due to cloud cover and shadows. This variability is illustrated in Figure 1, showing typical daily variation in solar illumination on a horizontal surface in Charlottesville, Virginia. This measurement includes the effect of typical cloud cover. Conventional IR thermography (ASTM D4788-03(2013), 2013) is practiced by mounting an IR camera to a vehicle and driving over a bridge deck. Video images of bridge deck surface temperatures are recorded and then examined, visually or with image analysis software, to identify temperature anomalies.

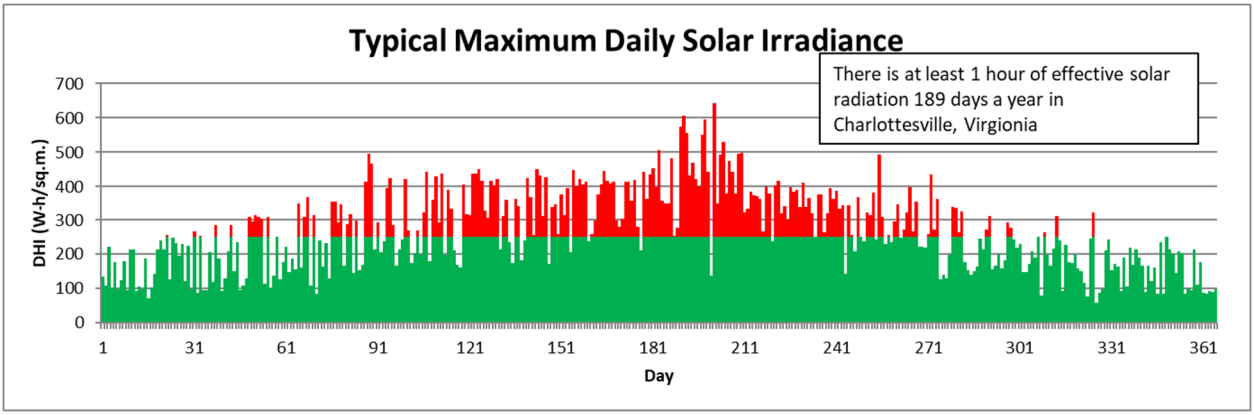

Figure 1. Typical daily variation in solar illumination on a horizontal surface in Charlottesville, Virginia

Simulations indicate that reliable differential temperature due to subsurface defects is obtainable when the maximum solar radiation level is 250 [W-h / m^2] or greater. For Charlottesville, this occurs only for about 30 percent of the daylight hours in a typical year. However, there are typically 125 days per year when there are a least three hours of effective solar radiation. These hours occur most frequently in the summer and between the hours of 9 AM and 3 PM. In Charlottesville, it is likely that thermography will not be effective for the months of October thru February. According to solar resource maps, produced for the U.S. Department of Energy (DOE) by the National Renewable Energy Laboratory (NREL), Virginia receives a range of annual average daily total horizontal solar irradiance of 4000 to 4500 [W-h / m^2 / day] (Gilroy 2017). Charlottesville is near the center of this range. South-east and Atlantic coastal areas are at the higher end of this range, while areas along the west state border are at the lower end of this range. Respectively, this may cause the number of effective days to increase or decrease slightly, when compared to Charlottesville.

In addition, convective heat transfer at the surface due to winds can greatly reduce the magnitude of the surface temperature. Surface emissivity variations of the bridge deck can also result in apparent temperature variations. It is very unlikely that conventional Thermography data acquisition, essentially an image with an exposure time of 1/30th of a second, will occur at the optimal time during the day when the temperature variations due to subsurface delaminations will be at a maximum. The presence of an overlay also has a significant effect on the IR data. The overlay is additional material which must be heated and through which the heat must conduct. This reduces the magnitude of the surface temperature effect due to a delamination. It also results in additional lateral diffusion, which spreads the temperature difference due to an anomaly over a greater surface area, resulting in a less distinct indication. A qualitative indication of the effect of a two-inch thick AC overlay on the temperature difference due to a defect two inches below the concrete surface is provided in Figure 2. The magnitude of the indication is significantly reduced and the total time when the temperature difference is greater than 1 degree (high probability of detection) is reduced by 25%. The probability of detecting such surface temperature anomalies using traditional thermography is correspondingly reduced.

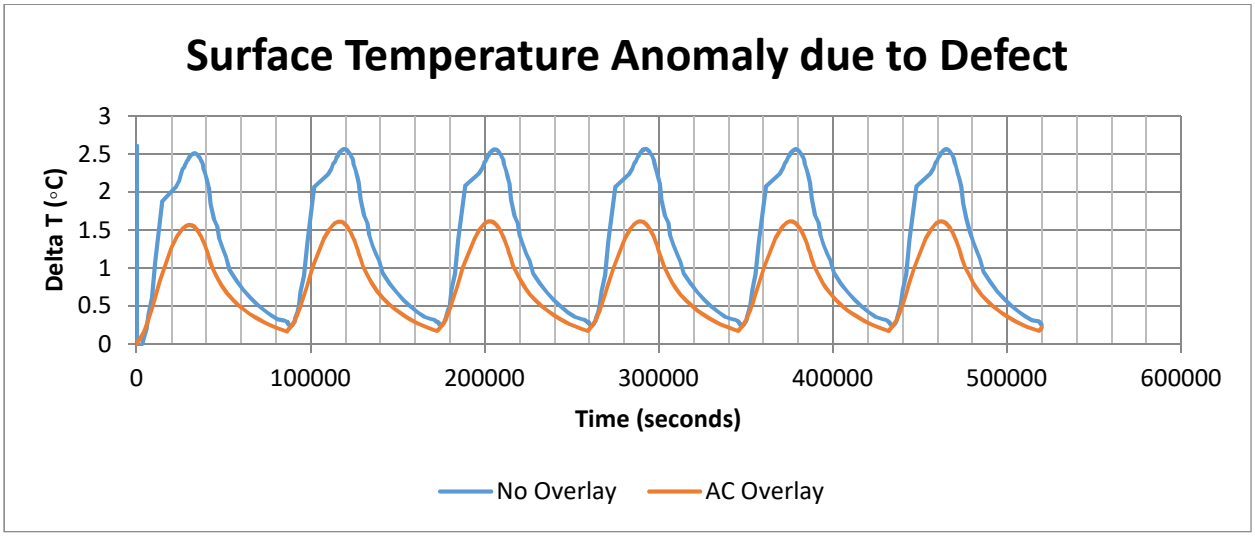

Figure 2. Surface Temperature Anomaly Plot

Time-Lapse Infrared Thermography

Many of the factors which reduce the reliability of traditional IR thermography can be addressed by a different approach to acquiring and analyzing IR data. The concept is to collect IR data over a much longer time period than traditional thermography. Typical thermography utilizes very short snapshots of IR data collected while driving over a bridge. The probability of collecting surface temperature data that is optimal is practically zero. However, collecting IR data over an extended period, hours or even days, greatly increases the probability of collecting data at the optimal time. The extended data acquisition time reduces the significance of random effects such as cloud cover and wind. This approach also greatly increases the sample of data that is acquired. Additionally, this approach offers the ability to apply physics-based data analysis to extract far more information from the acquired data than is possible with traditional IR data processing. It can provide quantitative thermal property data of bridge decks, and support objective defect detection rather than subjective analysis of images. This is the fundamental difference between the proposed use of thermography and the conventional approach.

PURPOSE AND SCOPE

The purpose of this research is to develop an improved method of applying infrared thermography, to the evaluation of bridge decks in Virginia. This improved method will be used to distinguish between concrete bridge deck delamination and overlay debondment defect types. It will also provide depth to delamination results.

The scope of this research is limited to non-experimental methods. A 3-dimensional simulation model will be created for the purpose of conducting parametric studies. These studies will focus on identifying key environmental factors to be considered during the development of a time-lapse infrared data acquisition system and software tool to analyze the acquired data.

METHODS

The research conducted consists of the following tasks:

- **Task 1** – Conduct a parametric investigation, using a 3-dimensional simulation model. The simulation model shall be a practical transient heat conduction simulation model representative of a typical concrete bridge deck subject to natural temperature and solar radiation cycles. The model shall be capable of simulating 3-dimensional heat flow, provide surface and internal temperature variation results, and include the effects of an overlay. This investigation shall focus on the effects of environmental factors. The results will be considered during the development of a time-lapse data acquisition system and quantitative analysis algorithm.
- **Task 2** – Develop a prototype time-lapse thermography data acquisition system. The data collected by this system will be used to directly support the further development of physics-based qualitative and quantitative analysis tools in the future.
- **Task 3** – Develop a quantitative time-lapse infrared data post-processing analysis tool. Using time-lapse infrared data, this tool will perform a physics-based quantitative analysis to distinguish between a concrete deck delamination and an overlay debondment. Additionally, it will provide depth to delamination results. This tool shall be bench-marked using the 3-dimensional transient heat conduction simulation model.

Task 1: Parametric Investigation

From the conceptual stages of this project, it was understood that a custom TLIRT system would need to be developed to acquire time-lapse data. Additionally, it was anticipated that the developed system would need to acquire multiple types of data, in addition to time-lapse IR data, to support a physics-based analysis. To identify and understand the types of data needed, a simulation-based parametric study was first conducted. To this end, a 3-dimensional finite element solid model representative of a concrete bridge deck with an overlay layer was created. The model, shown in Figure 3, was created using ANSYS Workbench, a physics modeling and

simulation software package, capable of simulating transient heat transfer problems with thermal (solar and emissive) radiation and convective boundary conditions. The identified simulation inputs were organized as being either heat transfer properties, environmental inputs or geometric parameters.

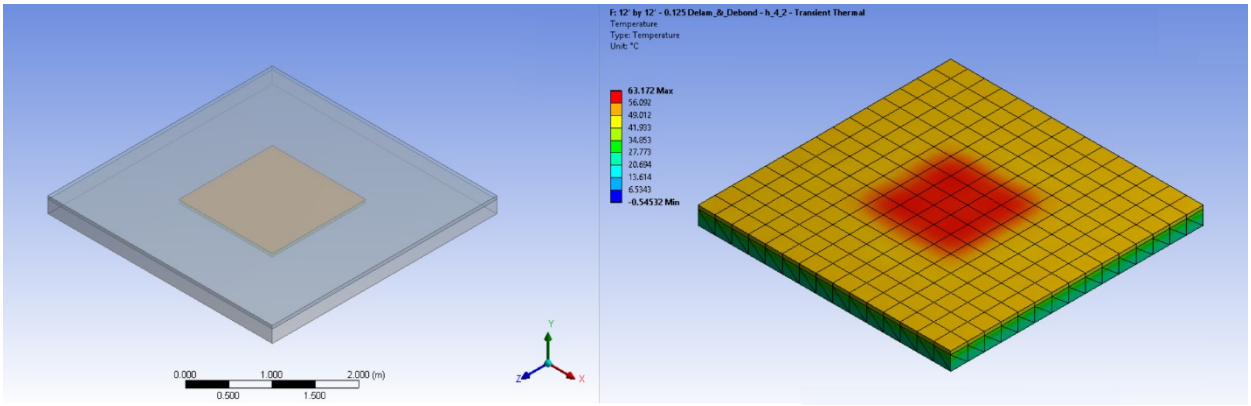

Figure 3. Finite Element Simulation Model Developed in ANSYS Workbench

Heat Transfer Properties

Heat is transferred in three ways, which include: radiation, convection and conduction. Radiation and convection are the mechanisms responsible for the transfer of heat into and away from a bridge deck at its surface; conduction is responsible for the transfer of heat through the bridge deck. There are two property types that affect heat transfer, they include: thermophysical and surface condition properties. Thermophysical properties are inherent material properties that typically are dependent on state variables (i.e., pressure, temperature, etc.). The applicable thermophysical properties, in the context of this research, affect conduction. These properties are shown in Equation 1, the transient heat conduction equation (without internal heat generation), also known as the diffusion equation. The heat conduction equation describes how temperature (T), evolves over time (t) as a function of the bridge decks thermophysical properties, density (ρ), specific heat (c) and thermal conductivity (κ). These thermophysical properties are relatively weak functions of their state variables; as such, their value variations over the expected exposure range were considered trivial. Consequently, these properties are treated and shown as constant values. While not used explicitly in the simulation, as is shown, the thermophysical property values may be lumped together into a single thermal diffusivity ($\propto$) value. Thermal diffusivity may be thought of as a measure of how quickly a material responds to temperature change. It should be clarified that a multi-layer system was simulated. This is because the simulated bridge deck included subsurface defects and an [asphalt] overlay system. Therefore, thermophysical properties for each layer of this multi-layer system were defined.

$$\frac{}{} + \frac{}{y} + \frac{}{z} = \frac{\rho c}{\kappa} \cdot \frac{}{t} = \frac{1}{\alpha} \cdot \frac{}{t} \qquad \text{Equation 1}$$

Radiation was identified to be one of the mechanisms that cause heat to transfer into and way from the bridge deck. All matter with a temperature above absolute zero emits radiation across all wavelengths of the electromagnetic spectrum. When dealing with heat transfer

applications, we are particularly interested in the radiation emitted in the thermal range of the electromagnetic spectrum (0.1 to 1000μm wavelengths). A bridge deck absorbs radiation emitted from the sun, the atmosphere and in general, all local matter. As contributions from local matter (e.g., trees, buildings, etc.) were considered trivial radiation sources, only solar and atmospheric radiation sources were considered. Furthermore, the bridge deck also emits thermal energy. The resulting net radiation energy balance is summarized as:

$$\begin{matrix} Net \\ Rad\ at\ on \\ Energy \end{matrix} = \begin{pmatrix} Solar \\ Rad\ at\ on\ Energy \\ Absorbed \end{pmatrix} + \begin{pmatrix} Atmospher\ c \\ Rad\ at\ on\ \ Energy \\ Absorbed \end{pmatrix} - \begin{pmatrix} Em\ tted \\ Rad\ at\ on \\ Energy \end{pmatrix}$$

A blackbody is a theoretical material that is characterized by its ability to perfectly emit and absorb radiation energy. The total amount of radiation a blackbody emits is defined by the Stefan-Boltzmann law, shown by Equation 2. This law provides a relationship between the total emitted radiation energy from a blackbody [material] and its absolute surface temperature, where the shown Stefan-Boltzmann constant (σ) is equal to $5.670\ \times\ 10^{-8}\ W/m^2 \cdot K^4$.

$$\dot{q}_b = \sigma T_{b,surf}^4 \qquad \text{Equation 2}$$

The bridge deck is not a blackbody. That is to say radiation is not perfectly absorbed or emitted by it. Based on this understanding, the net energy balance summarized earlier can be expressed by Equation 3. This equation defines the net rate of radiation heat transfer; that is to say the net radiation flux.

$$\dot{q}_{ra\ ,net} = \alpha_s G_{solar} + \alpha_a \sigma T_{atm}^4 - \varepsilon \sigma T_{surf}^4 \qquad \text{Equation 3}$$

The first term in Equation 3 is the amount of total incident solar radiation absorbed by the bridge deck. The second term is the amount of atmospheric radiation absorbed by the bridge deck, for an [absolute] atmospheric temperature (often called the sky temperature). The final term is the amount of radiation emitted from the bridge deck into the atmosphere, for an [absolute] surface temperature. Each term is scaled by surface condition dependent heat transfer property, having a value between zero and one. These properties that account for the fact that neither the bridge deck nor the atmosphere is a blackbody include emissivity (ε), atmospheric absorptivity (α_a) and solar absorptivity (α_s). Emissivity quantifies the fractional amount of radiation emitted by the bridge deck, relative to that which would be radiated by a blackbody having the same surface temperature. Atmospheric absorptivity is used to quantify the fractional amount of atmospheric radiation being absorbed by the bridge deck. Solar absorptivity is used to quantify the fractional amount of solar radiation being absorbed by the bridge deck. Due to differences in [electromagnetic] spectral distributions, solar and atmospheric absorptivity values often differ. As expressed in Equation 4, two simplifications are made to Equation 3. First, using Kirchhoff's Law the atmospheric absorptivity is set equal to the emissivity ($\alpha_s = \varepsilon$). Second, as the absolute atmospheric (or sky) temperature does not deviate too much from the ambient temperature, the [absolute] ambient air temperature ($T_\infty = T_{atm}$) is substituted.

$$\dot{q}_{ra\ ,net} = \alpha_s G_{solar} + \varepsilon\sigma(T_\infty^4 - T_{surf}^4) \quad \text{Equation 4}$$

Convection was identified to be the second of two mechanisms causing heat to transfer into and way from the bridge deck. As shown in Equation 5, the convective heat flux is expressed by Newton's Law of cooling. The direction of the heat transfer is dependent on the sign of the temperature change. Therefore, if the surface temperature of the deck is greater than that of the surrounding ambient air temperature, then heat is transferred away from the deck. The rate of heat transfer is affected by the convective heat transfer coefficient (h_{conv}); this is not a fixed or even constant property. This property is often determined experimentally or measured. However, for the purpose of the parametric study averaged values were assumed for the top and bottom surfaces of the bridge deck.

$$\dot{q}_{conv} = h_{conv}(T_{surf} - T_\infty) \quad \text{Equation 5}$$

Convection by a free system, like a bridge deck, actually includes a combination of conduction and random [air] fluid motion processes. At the surface/air interface heat is transferred into or away from the deck by through the conduction of heat between the deck and contacting air molecules. However, further away from the surface/air interface these air molecules are transported by natural buoyancy and forced wind driven currents (i.e., mixed convection). The speed and direction with which these currents pass over the surface/air interface has an effect on the rate at which the deck will heat or cool convectively. Therefore, deck geometry and wind velocity play a large part in the value of the convective heat transfer coefficient. Average convective heat transfer coefficient values for the parametric study were determined using empirical formulas developed for flat plates. An example calculation used to arrive at these values can be found in the Appendix. To summarize the relevant heat transfer properties, and display the values assumed, Table 2 is provided. These values were compiled from various sources (Cengel 2011, Chadbourn 1996).

Table 2. - Thermal Property Values Assumed

Property	Units	Concrete	Asphalt	Air
Density	kg / m^3	2300	2353	1.164
Specific Heat	J / kg K	880	870	1007
Thermal Conductivity	W / m K	1.4	1.06	0.026
Solar Absorptivity	Unitless	0.60	0.90	----------
Emissivity	Unitless	0.90	0.90	----------
Avg. Convective Heat Transfer Coefficient (Top Surface)	W / m^2	----------	4 (Low) 21 (High)	----------
Avg. Convective Heat Transfer Coefficient (Bottom Surface)	W / m^2	2 (Low) 21 (High)	----------	----------

Environmental Inputs

Environmental data was necessary to perform the simulated parametric investigation. By inspection of Equation 4, two required environmental inputs include total incident solar radiation (G_{solar}) and ambient air temperature(T_∞). The total incident solar radiation, as expressed by Equation 6, is the sum of the direct solar radiation (G_D) normal to the bridge decks

surface, assumed to be horizontal, and the uniformly scattered diffuse solar radiation(G). This solar radiation measurement is termed the diffuse horizontal irradiance (DHI).

$$G_{solar} = G_D \cos\theta + G \qquad \text{Equation 6}$$

Figure 4 shows a plot of the total incident solar radiation, total absorbed incident solar radiation and ambient air temperature applied to the simulation, over a single day. One source states that due to atmospheric attenuation, of the nearly 1373 $[W/m^2]$ of total solar irradiance which enters the earth's atmosphere, on a clear day only about 950 $[W/m^2]$ will reach the surface of the earth; this attenuation is caused by atmospheric absorption and scattering. When the sky is not clear this amount can go down considerably. Consequently, it was assumed that the peak total incident solar radiation was 600 $[W/m^2]$. As shown, the incident solar radiation was modeled as a sinusoidal function, with non-zero, positive values occurring over a 12-hour day-time duration; the peak value ($G_{solar} = 600\ [W/m^2]$) occurring at noon. The 12-hours of assumed solar contribution corresponds to a daily average of approximately 380 [Wh/m^2] of irradiation. As discussed earlier (see Figure 1) this is an appropriate value for Charlottesville, Virginia. For the purposes of heat conduction modeling, the incident solar radiation is scaled down by the absorptivity of the wearing surface material. During the remaining 12-hour night-time duration, the total incident solar radiation was taken to be zero ($G_{solar} = 0\ [W/m^2]$). Ambient temperature was also modeled as a sinusoidal function, with a 24-hour period. Also shown in the Figure 3, the peak-to-peak low and high values were $60[°F]\ to\ 90[°F]$ (approximately $15.6[°C]\ to\ 32.2[°C]$) respectively, with the peak high value occurring at noon.

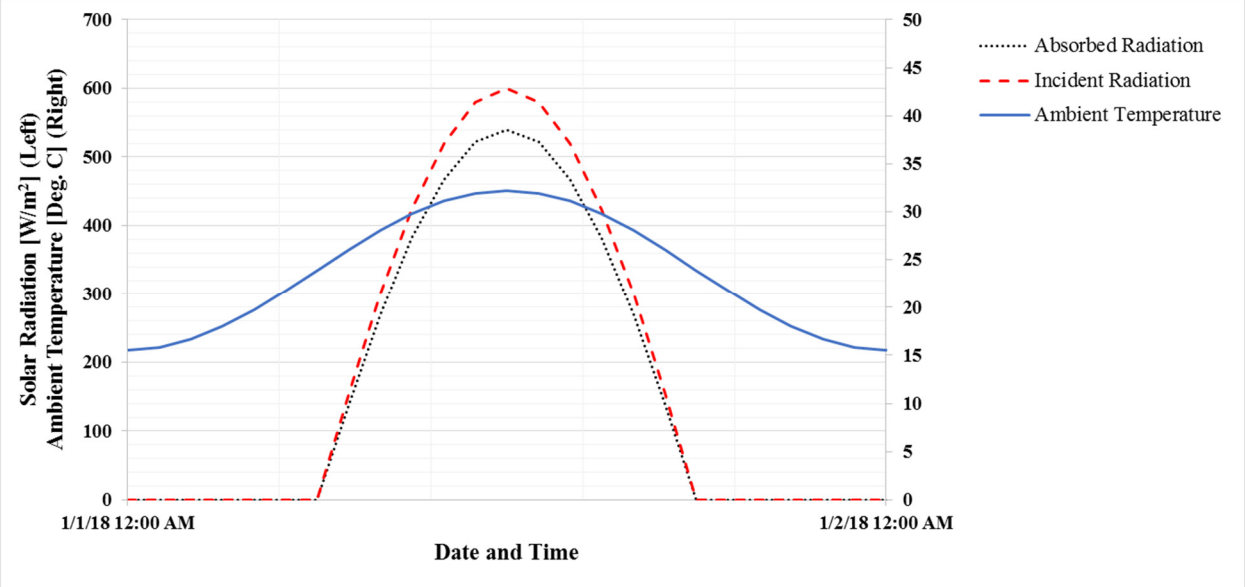

Figure 4. Simulation of Environmental Inputs

Geometric Parameters

The following geometric parameters were selected. The length and width of the solid model was 12 [ft.] by 12 [ft.] (3.6 [m] by 3.6 [m]). The thickness of the concrete deck was 8[in.] (20.3 [cm]). The thickness of the asphalt overlay was 2 [in.] (5.1 [cm]). The model did not

incorporate a stay-in-place formwork layer. Additionally, the model was not complicated by the inclusion of embedded reinforcement material or supporting members (e.g., beams or girders). Delamination and debondment defects were each modeled to have a length and width of 5 [ft.] by 5 [ft.] (1.5 [m] by 1.5 [m]); they each also were given a $1/8^{th}$ [in.] (0.3175 [cm]) thickness; the delamination depth location varied.

Task 2: Time-lapse Infrared Data Collection System

A prototype TLIRT system was acquired for this research project; the version of the delivered system can be seen in Figure 5. The system TLIRT was developed by FCI/ThermalStare and is called the IR Ultra-Time Domain (IR-UTD) imaging technology. For a more detailed description of the IR-UTD system, its capabilities and developer contact information, the reader is referred to a report prepared by Glenn Washer, P.E., PhD, and others with the University of Missouri, for the Missouri Department of Transportation (MoDOT report number cmr 16-007). The report is entitled "Field Testing of Hand-Held Infrared Thermography, Phase II". A brief overview of the acquired system follows.

The developed TLIRT system collects several types of required time-lapse data. The first two types of required data included time-lapse IR and digital image data of the bridge decks wearing surface. The acquired system comes equipped with an IR and digital image camera. Both cameras fit into a single camera housing with an attached programmable pan-tilt assembly. The camera housing (with pan-tilt assembly) is attached to a telescopic mast, which may be extended up to 30 [ft.]. The system also has a weather-proof control box with a field central processing unit (CPU). The CPU controls the camera pan-tilt positioning, time-lapse digital and IR image acquisition and data storage. The TLIRT system also is equipped with an integrated weather station. The weather station collects environmental data that is critical for a physics-based analysis. The collected environmental data includes ambient temperature, wind velocity, solar radiation (combined direct and diffuse) and rain event data. Another function of the CPU is to control the weather station setup and scheduled data downloads, this prevents possible data overwriting. Also, using a common CPU permits time-stamp synchronization.

Figure 5. IR-UTD System Deployment

Practical aspects of systems deployment were also considered. As mentioned, the TLIRT system's camera housing has a programmable pan-tilt assembly. This permits the user to optimize the amount of observable surface area per set-up, reducing the total number of set-ups required. The TLIRT system was designed to be deployed using parapet mounting clamps. This makes possible the deployment of the system nearly anywhere along the bridge span, whether or not a wide shoulder is available. The parapet mounted design means that traffic control is only needed during deployment, repositioning and system recovery operations. The system is powered by a rechargeable battery pack, housed in a weather-proof field box. The rechargeable battery pack can power the system for approximately two days. However, the exact maximum duration depends on several power usage factors, such as data acquisition rate and the number of camera positions programmed. If available, the system may also be connected to an onsite AC power source (e.g., power outlet or generator) with the battery pack serving as a backup.

Task 3: Physics-Based Analysis Tool

Algorithm Introduction

Consider a bridge deck with known heat transfer properties, boundary conditions (e.g. solar radiation, ambient temperature, etc.) and a defect configuration (e.g., depth to a delamination). With this information a transient conduction heat transfer simulation could be performed, producing a simulated surface temperature response record for any location of interest on the simulated surface. In the context of this research, the surface location of interest would be a location on the bridge deck directly over a suspected subsurface defect. The simulated surface temperature response would be the solution to this heat conduction problem. In practice, the defect configuration is unknown and the surface temperature response record at a location of interest can be observed. In this case, the type of problem one is most interested in solving is called an inverse heat conduction problem.

An identification algorithm which solves this type of problem was designed. If the heat transfer properties, boundary conditions and a surface temperature response record are known, then the defect configuration beneath the surface temperature response record may be determined. In essence, the surface temperature response record is treated like a "finger print", which can uniquely identify a specific defect configuration. The identification algorithm designed employs a heuristic, discretized trial-and-error simulation approach, making tractable the convergence upon defect a solution having a seemingly infinite number of possible candidate trial permutations. The identification algorithm has three distinct phases, which are described later, and is built around a numerical implicit transient heat transfer conduction (HTC) model. Three input classes are passed into the HTC model, which include: general, IR time-lapse and variable input classes. A brief description of the algorithm's inputs is provided next.

Algorithm Inputs

General Inputs

General input data consists of environmental, thermal property and geometric data. Environmental data includes local total incident solar radiation and ambient air temperature data records. During field deployment, these data records are acquired by the TLIRT system's integrated weather station. The environmental data records are sampled at a rate sufficient to be representative of the actual evolving local weather, spanning the entire observational duration.

Thermal property data is the second type of general input data, consisting of material layer and surface thermal property data. For each possible material layer of the bridge deck's cross section the [programs] user provides density, specific heat and thermal conductivity values. Material layers may include the concrete deck, an overlay system, formwork and any defects (i.e. delaminations and debondment). These thermal property values are used, by the program to calculate the thermal diffusivity for each layer. Additionally, the user may specify a thermal contact conductance (TCC) value for defect permutations that include contact defects. Surface thermal property data includes the solar absorptivity and convective heat transfer coefficients. These values are determined by the algorithm during first two phases of the algorithm. However,

if known, the user may choose to supply this data, bypassing the algorithms first two phases; this can greatly reduce the total computational time of the analysis.

Geometric data of the idealized bridge deck cross-section is the third type of general input data. This geometric data includes the nominal thickness for each of the ideal (i.e. defect free) cross-sectional material layers. That is to say, in this input section, the user provides all the nominal layer thicknesses, except for that of defect layer(s). Geometric parameters for defects are set by the user as part of a variable class input, discussed later. Nominal layer thicknesses data is generally obtained from as-built plans or other means.

IR Time-Lapse

The IR time-lapse class of input data includes the observed surface temperature response record for each surface point location of interest. This data record is generated by the TLIRT system. There are two types of response records used by the algorithm; the records include ideal and defect response records. Ideal response records are those records corresponding to locations on the bridge deck where there is high confidence that a subsurface defect does not exists. Ideal response records are used in the first two phases of the identification algorithm, to determine the material surface properties (i.e., solar absorptivity and convective heat transfer values) which are not required from the user. Defect response records are those records corresponding to locations on the bridge deck where there is high confidence that a subsurface defect does exists. Defect response records are used later in the third phase of the identification algorithm to identify a specific defect configuration.

Variable

The variable class of input data is the final class of inputs, consisting of the simulation start time, duration, discretization interval, and defect scenario data. Additionally, until the surface thermal property data is finalized at the end of phase two or provided by the user, solar absorption and convective heat transfer values are considered part of this variable class. The start time along with the simulation duration, are used to locate and generate all subsets of data records, prior to being passed into the HTC model. Interestingly, based on the simulated 6:00 am sunrise, it was found necessary for the data collection start time to begin in the morning between 8:00 a.m. and 9:00 a.m. This is because the initial temperature profile guess, required by all numerical models, is assumed constant and equal to the observed surface temperature corresponding to the start time. The simulation study suggests that in the morning hours between 8:00 a.m. and 9:00 a.m., or between two and three hours after sunrise, the internal temperature profile is nearly constant. For practical purposes, as the actual time of sunrise varies with the time of the year, the start time window may need to be adjusted. The discretization interval, used in phase two, is provided by the user to create the discretized top surface convective heat transfer function. The smaller the discretization interval selected, the closer the discretized function comes to looking like the actual function. However, there is a definite trade-off in the amount of computational time required when selecting smaller intervals; the smaller the interval selected, the more computational time required. As mentioned before, the algorithm employs a heuristic, discretized trial-and-error simulation approach; therefore, candidate defect scenarios need to be supplied to the HTC model. The algorithm was designed to consider four types of defect scenarios, which include:

- **Scenario 1** – Total defect free condition
- **Scenario 2** – Debondment of an overlay system, with the underlying decking system remaining defect free.
- **Scenario 3** – Single horizontal delamination of the decking system, with an overlay system remaining defect free.
- **Scenario 4** – Combined debondment of an overlay system and a single horizontal delamination of the decking system.

The program automatically passes each required scenario into the HTC model, which includes user defined defect parameters. The defect parameters selected include the range of defect thicknesses and the defect depth search envelope to be considered. Depending on the scenario being considered, the number of defect thickness and location permutations will vary.

Algorithm Phase One

As mentioned, the identification algorithm is organized into three phases. The purpose of the first phase is to determine the solar absorptivity and average convective heat transfer values for the top and bottom surfaces; the algorithm used is shown by the diagram in Figure 6. Phase one begins by loading the HTC model inputs into the HTC model. It should be noted that the inputs include a hard-coded initial guess for the average convective heat transfer values and only the first defect scenario. Recall that the first defect scenario provides the ideal (or defect free) cross-sectional configuration.

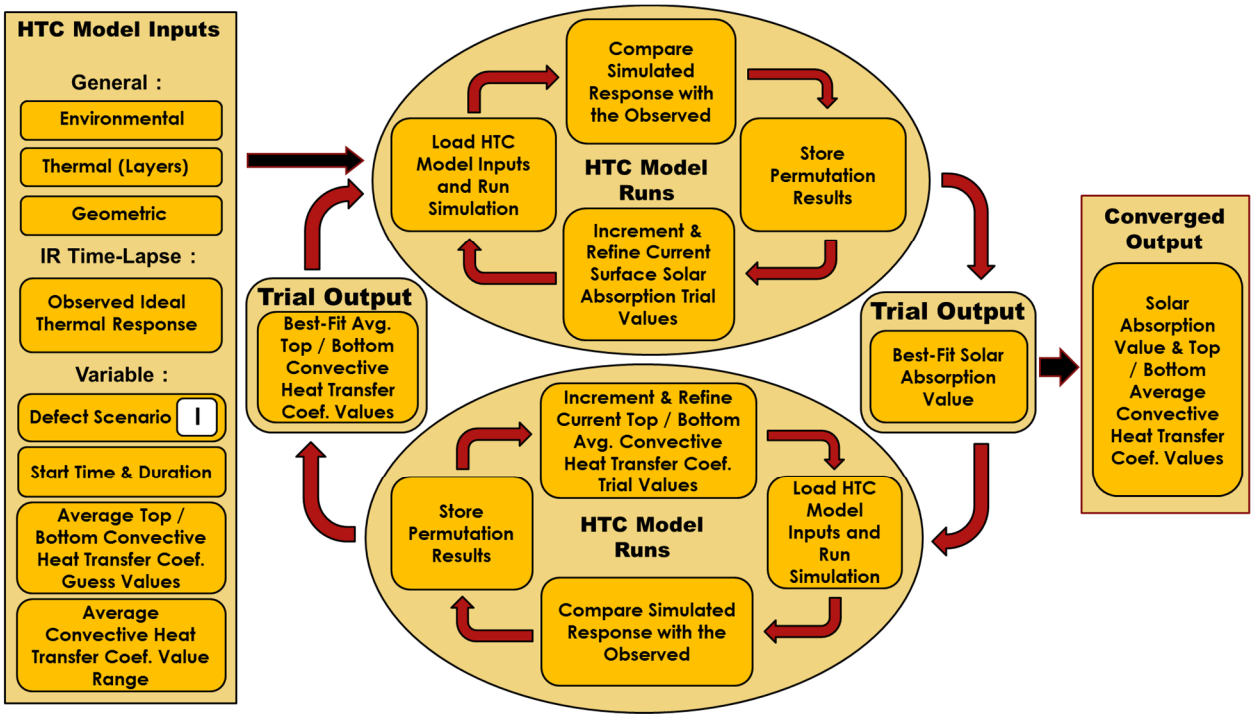

Figure 6. Identification Algorithm, Phase 1

Using the hard-coded initial guess, a trial solar absorption value is assigned by the algorithm. This provides the HTC model with all the inputs required to start the simulation. The surface temperature results from the simulation are compared to the observed ideal surface

response corresponding to a location on the bridge deck where there is high confidence that a subsurface defect is not present. The variance is determined and is stored along with the corresponding solar absorption trial value. The solar absorption trial value is then varied and a new HTC model is run. This first looping process is carried out across the total range of trial solar absorption values (0 to 100 percent). The permutation with the smallest variance is identified and the corresponding solar absorption value is passed forward into a second HTC model loop. The second loop fixes the trial solar absorption value, and average convective heat transfer values are systematically varied across a range of values, provided by the user. Similar to the first loop, the modeled surface temperature response is compared to the observed ideal response and variance values are determined. The average convective heat transfer value pair with the smallest variance is passed back to the first HTC model loop. This iteration back and forth between the two loops continues until the change in the best-fit solar absorption value falls below a user specified tolerance. When the iteration concludes, the first phase will have identified the most likely solar absorption value and the corresponding average convective heat transfer coefficient values. Should the user prefer to use a convective heat transfer coefficient function, rather than a single average value, the output values from phase one are passed into phase two for further analysis.

Algorithm Phase Two

The purpose of the second phase is to determine a discretized convective heat transfer coefficient function for the top surface; the algorithm used is shown by the diagram in Figure 7. The reason for omitting the determination of a function for the bottom surface is due to the following assumption. It is assumed that girders impede the motion of both forced and naturally buoyant convective air currents along the bottom surface of the decks. Consequently, not only will the actual values be relatively small, any variations should be trivial. Therefore, it is reasonable to conclude that the bottom surface average convective heat transfer coefficient, determined by the identification algorithm during the first phase, may be applied across the entire duration of the simulation.

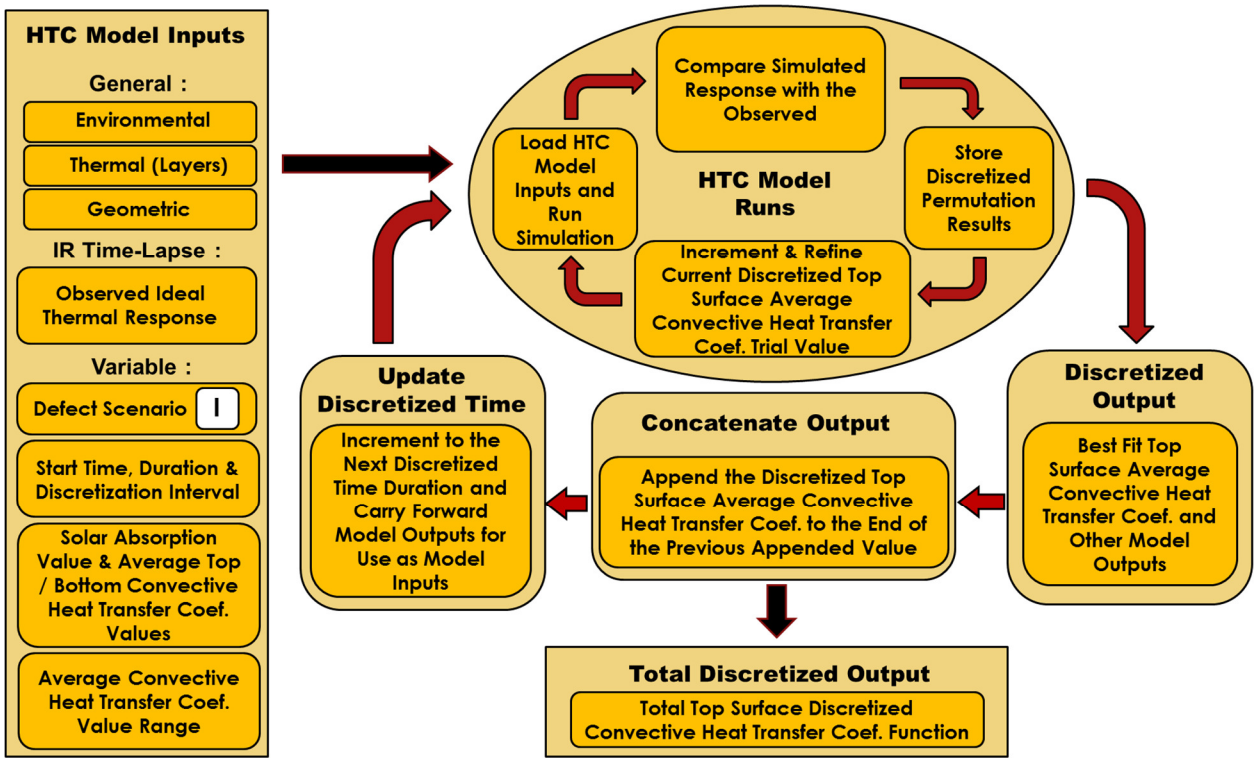

Figure 7. Identification Algorithm, Phase 2

Phase two begins by loading the HTC model inputs into the HTC model. It should be noted that the inputs include the user specified discretization interval, solar absorption and the top and bottom surface average convective heat transfer coefficient values, determined by the first phase. Similar to the first phase, this second phase also only requires the first defect scenario. The HTC model runs the simulation over the discretized time interval, beginning at the starting time. The simulated surface temperature results for the discretized time interval are compared to the observed ideal surface temperature response corresponding to the same time interval, at a location on the bridge deck where there is high confidence that a subsurface defect is not present. The variance is determined and is stored along with the corresponding discretized top surface average convective heat transfer coefficient trial value. The trial value is then varied and a new HTC model is run; this looping continues until all trial values are systematically varied across the range of values, provided by the user. The permutation with the smallest variance is identified and the corresponding discretized top surface average convective heat transfer coefficient value is passed to a list for appended values. All required outputs from the current discretization interval are passed forward for use as initial values in the next discretization interval. This second algorithm phase continues until discretized top surface average convective heat transfer coefficient values are determined over the entire defined duration. An interpolant function is created from the list of appended values.

Algorithm Phase Three

The purpose of the third and final phase is to identify the defect cross-sectional layer configuration, beneath the surface location of interest on the bridge deck; the algorithm used is shown by the diagram in Figure 8. The location of interest selected by the user should correspond to a location where there is high confidence that a subsurface defect exists. The goal is to identify the most probable defect type and its depth, beneath the location where a defect is suspected to be. Areas of suspected subsurface defects may be identified using the basic qualitative program provided by the manufacturer of the TLIRT system used in this report, or another NDE method. It should be noted that the manufacturer of the TLIRT system does offer advanced qualitative post-processing for the IR time-lapse data collected. However, this does not exclude the independent development of advanced post-processing tools or applications by others.

Phase three begins by loading the HTC model inputs; these inputs now also include the thermal surface data, determined by the first two phases, and all applicable defect scenarios. The HTC model runs the simulation for the specified duration, using a trial defect permutation belonging to the current defect scenario type. The surface temperature results from the simulation are compared to the observed defect surface response corresponding to a location on the bridge deck where there is high confidence that a subsurface defect is present. The variance is determined and stored, along with the permutations defect parameters. The trial permutation is then systematically varied and a new HTC model is run; this looping process continues over the user's range of defined defect parameters. Once the range of applicable permutations for the current defect scenario type has been exhausted, the permutation with the smallest variance is identified and is stored. Then the next defect scenario is passed into the HTC model, and so on, until all the applicable defect scenarios have been simulated. Finally, each of the best-fit permutations for each of the applicable defect scenarios is compared. The permutation with the overall smallest variance is selected to be the most probable defect.

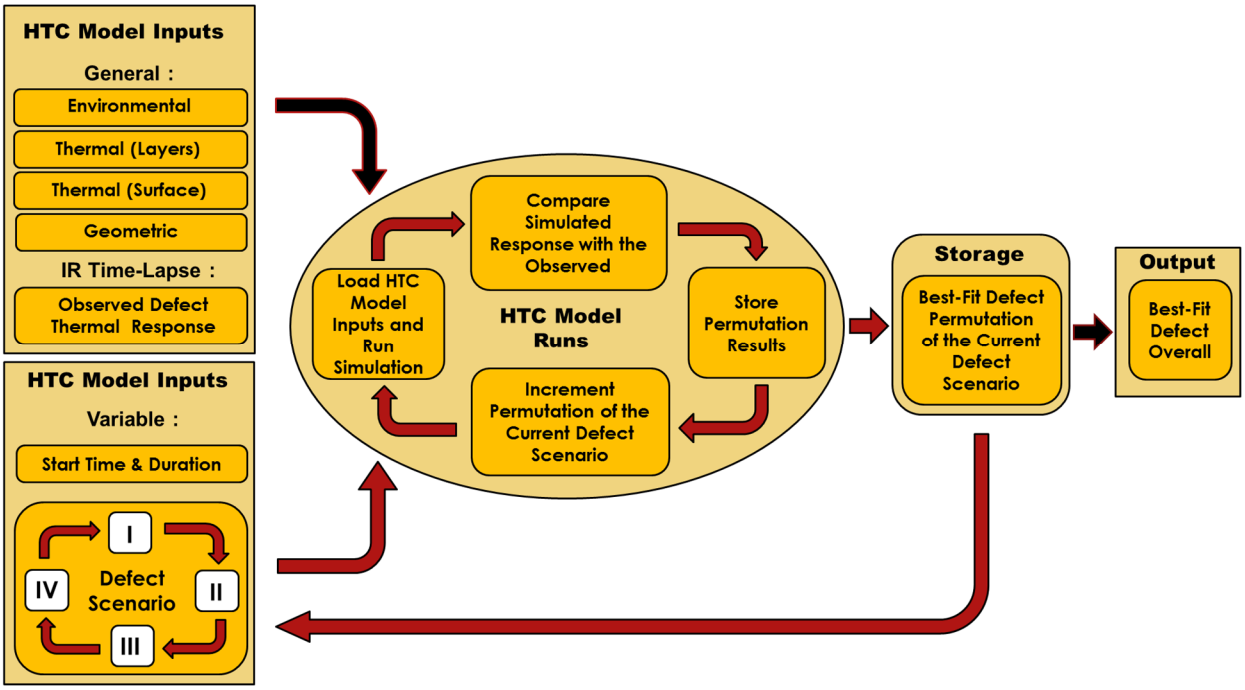

Figure 8. - Identification Algorithm, Phase 3

Physics-Based UHC Program

This section does not serve as a user's manual and therefore does not demonstrate the operation of the developed Unsteady Heat Conduction program (UHC program). Rather, it serves as a brief introduction to its user interface and highlights several features. However, this program may be equipped with a library of video tutorials, at a later date for training purposes. The physics-based program was developed in MATLAB (R2016b) and has a simple graphical user interface (GUI). Once the program is launched and the materials library is imported, the main GUI page, as shown in Figure 9, is visible.

The user interface is divided into four general input areas, including control, materials library, properties and output. The control inputs consist of the user start-time and duration fields. This is also where a file name is assigned and the program is started. Quick settings, are also located in the control section; they are provided to make the program's operation more user friendly. The last run feature loads all the settings used during the prior run. The launch UTD analysis is a convenient way to access a modified version of the qualitative program provided with the purchase of the IR-UTD system. The basic materials library is provided which stores thermal property data for various materials. This library may be easily updated or revised by the user. The properties input area is where the user defines the nominal thicknesses of each layer in the ideal cross-section and assigns material thermal properties from the materials library. In both the control and properties sections there are advanced settings, which need to be reviewed by the user prior to operation. Most of the advanced settings may only need to be set up once. The output area provides an operational status window, which provides instructions and notifications to the user during the analysis. When the analysis has completed, a description of the findings is displayed along with two dynamic plots of the results. The first plotted result is the simulated dynamic temperature profile, through the thickness of the cross-section, at the location of

interest. The second plotted result is a dynamic plot of the simulated surface temperature and the observed surface temperature at the same location. Neither are shown in Figure 9.

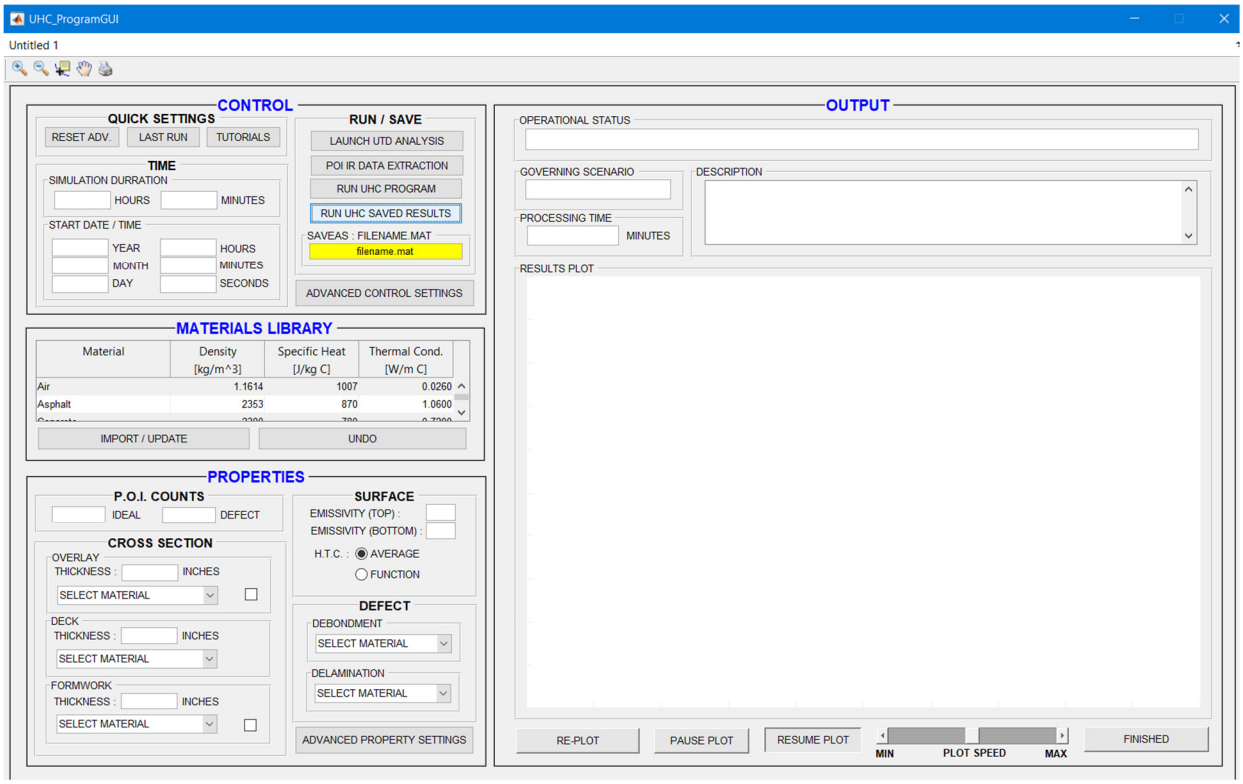

Figure 9. - UHC Program

RESULTS AND DISCUSSION

Task 1: Parametric Investigation

As shown in Figure 10, one simulation study looked at the general surface temperature response characteristics for given defect types over simulation duration of five days (four shown). This confirmed that the closer the defect is to the surface, the greater the surface temperature response deviates from the no defect scenario. It also confirmed that the greatest temperature deviation occurs when a combination of shallow deck delamination and overlay debondment occurs simultaneously. Interestingly, it was observed that the system took approximately three days to synchronize. This had to do with the initial temperature guess provided to the simulation. Numerical models require that an initial temperature of the system being modeled is assumed. In the case of this study, the initial guess was a uniform 32 [ºF] (0 [ºC]). However, if a nearly synchronized internal temperature profile could be guessed at the start of the simulation, then the system would not require much time to achieve synchronization. This realization is what leads the physics-based program, discussed later, to require that the simulation start time begin between two and three hours after sunrise. It was observed during this time window that the internal temperature profile was sufficiently uniform and could be assumed approximately equal to the surface temperature.

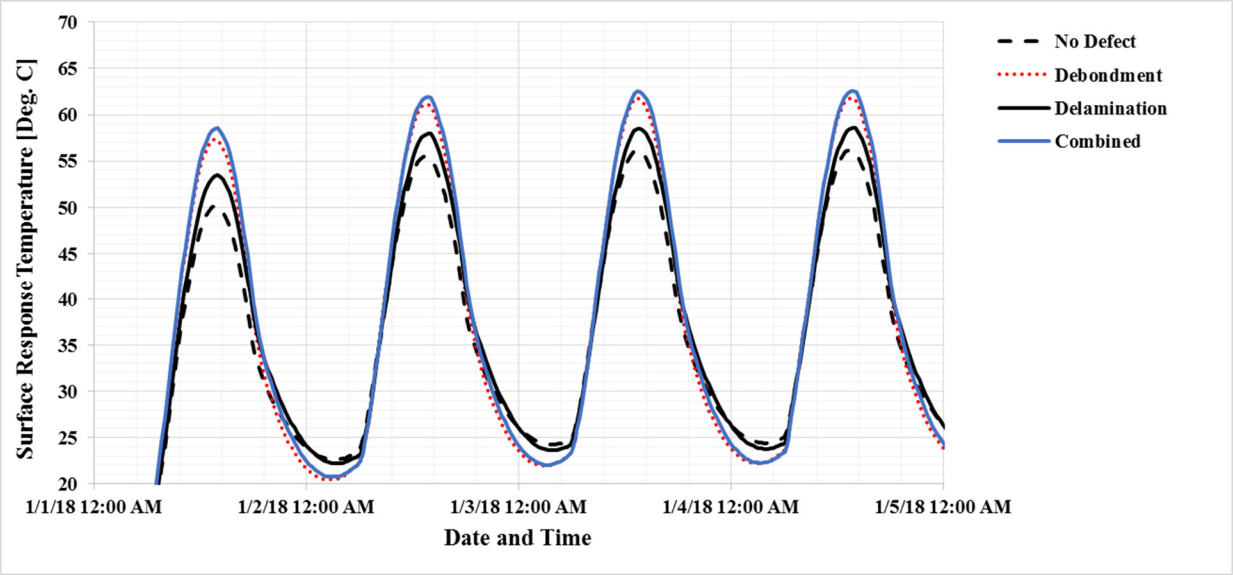

Figure 10 - Surface Temperature Response Per Defect Type

Another study (not illustrated) looked at the effect of sustained elevated wind velocity. In practice, IR thermography is not applied when the sustained wind velocity exceeds 10 [mi/h] (16 [km/h]) (ASTM D4788-03(2013), 2013). Calculations indicate that this corresponds to an average convective heat transfer coefficient of approximately 21 [W/m^2 K] (see Appendix). Assuming that the bottom surface would be shielded from the wind by the structural members, it remained at 2 [W/m^2 K]. This led to the finding that the overall temperature of the deck had lowered. Furthermore, the temperature response deviations from the no defect scenario were also greatly reduced. Based on this, during observational periods with sustained high velocity winds, it would seem unlikely that anything other than the shallowest of defects would produce noticeable anomalous temperatures areas.

Task 2: Time-lapse Thermography Data Collection System

The acquired IR-UTD system has been deployed on in-service bridge structures. While the data collected by the system has not been presented in this report, it should be stated that the system does work and is ready to support future research recommendations.

Task 3: Physics-based Analysis Tool

The results from UHC program analysis are shown in Figure 11. A 3-dimensional finite element heat transfer simulation was run. The geometric and material parameters used were similar to those used in the parametric study, except that the peak absorbed solar radiation was 340 [W/m^2] (not 540 [W/m^2]) and the emissivity value of one was used. The temperature response and environmental inputs used were entered into the UHC program. The UHC program was able to correctly identify the delamination cross-sectional thickness of 0.125 [in.] and its depth location of 4 [in.] below the asphalt. The plotted results correspond to the identified defect cross-sectional configuration determined to be most probable by the UHC program.

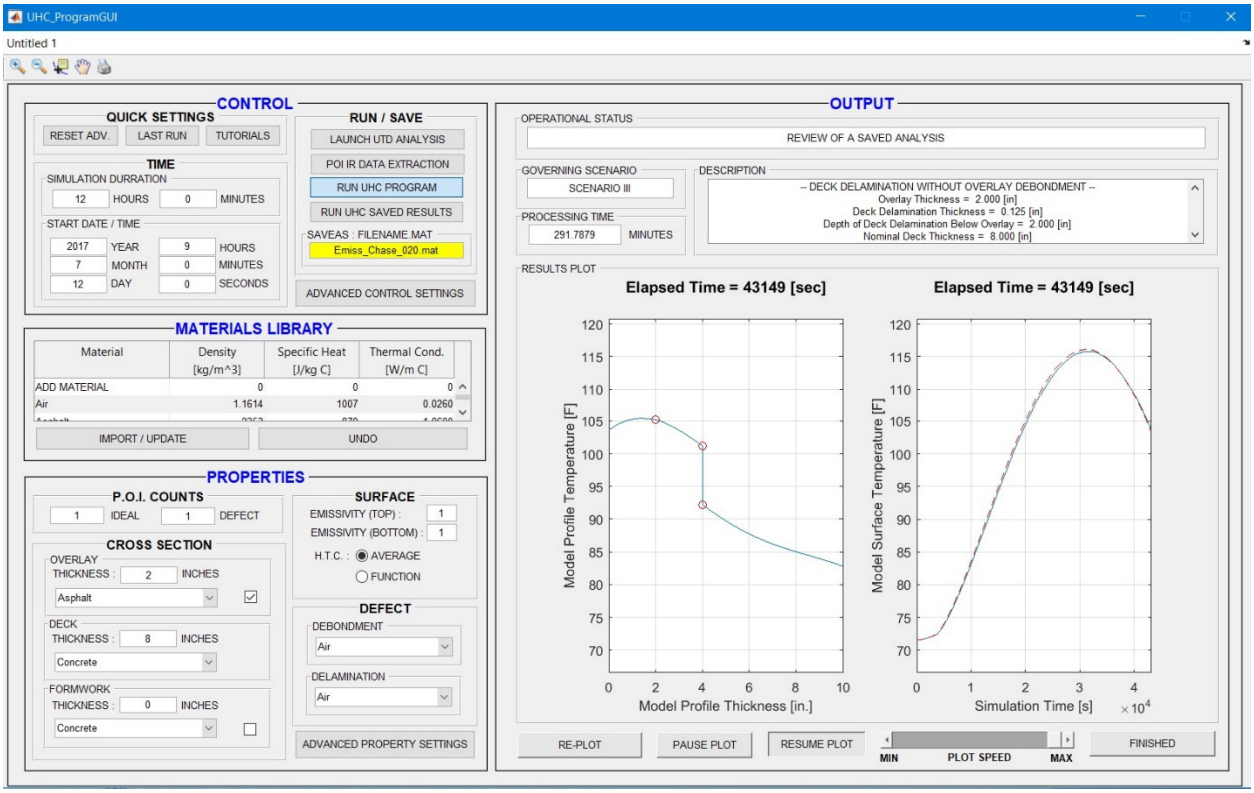

Figure 11. UHC Program Simulated Result

The left plot uses red circles to indicate material changes and to mark the corners of temperature discontinuities created by a defect. The right plot uses a solid blue line to plot the determined, simulated surface temperature. The red dashed line is used to plot the "observed" temperature response. In this case the observed temperature response is the output temperature response from the 3-dimensional finite element heat transfer simulation. For results using a more developed qualitative program, the reader is again referred to the report prepared by Glenn Washer, P.E., PhD, et al. (2016) with the University of Missouri, for the Missouri Department of Transportation (MoDOT report number cmr 16-007). The report is entitled "Field Testing of Hand-Held Infrared Thermography, Phase II".

CONCLUSIONS

- *On the qualitative front, Time-Lapse Infrared Thermography can reliably and accurately detect sub-surface delamination in reinforced concrete.*

- *On the quantitative front, using the innovative physics-based analysis program developed in this study, augmented Time-Lapse Infrared Thermography can detect the depth of delamination in reinforced concrete, which cannot be determined using traditional infrared thermography method.*

RECOMMENDATIONS

1. *VTRC should field-validate the qualitative Time-Lapse Infrared Thermography system for detecting delamination.*

2. *VTRC should field-validate the qualitative Time-Lapse Infrared Thermography system with the physics-based analysis program on field structures prior to production level deployment.*

IMPLEMENTATION AND BENEFITS

Implementation

With regards to recommendation 1 and 2, SPR-approved research study titled, *Reliability of Nondestructive Technologies for Evaluation of Bridge Decks,* has been initiated by VTRC to field validate the Time-Lapse Infrared Thermography System along with several other nondestructive evaluation technologies.

Benefits

User Benefits

The TLIRT system is a non-contact NDE tool designed with features that minimize impacts on traffic flow during deployment. In terms of traffic control, at most, single lane (or shoulder) closure is required during deployment, repositioning and system recovery operations. An experienced operator can deploy the system in less than an hour. During systems operation, traffic is permitted to flow un-impacted. The number of repositioning operations is minimized by the 30 [ft.] mast and camera housing pan-tilt feature. The system is battery powered and does not need to rely on an external power source. The parapet clamp design makes the technology highly deployable on most bridges. The IR full-field deck survey may be performed without removal of the overlay system. The full-field time-lapse data may be stored for future analysis. In the event, that an analysis needs to be conducted on a different deck location, a follow up deployment should not be required. Analysis of the collected data is not limited to the post-processing tools provided; collected data may be analyzed in-house or by consultants who have developed more advanced post-processing methods. Finally, the field CPU allows for future system expansion and upgrades, this may occur if there is a future need for another type of data or if there is a need to upgrade an existing component.

Cost Benefits

The reader will note that one of the report recommendations calls for additional steps of research. It is not possible at this time to predict how extensive a role the employment of time-lapse infrared thermography will play in the VDOT pavement maintenance program, nor is it

possible to predict how much TLIRT will improve the agency's ability to detect and measure delamination at various depths. It is clear, however, that TLIRT has something to contribute.

It is clear that when delamination is confined to the upper two or three inches of a concrete deck – that is, above the top level of the rebar frame – the typical rehabilitation involves removal of the damaged concrete by milling, followed by replacement with fresh low-permeability concrete. When delamination extends lower – that is, beyond the top of the rebar frame – then rehabilitation, if it were economical at all, involves removal of the damaged concrete by hydro-milling (hydro-demolition), followed by replacement with fresh low-permeability concrete.

Historical Estimate of the Unit Cost of Hydro-Demolition and Replacement

A search of the recent VDOT bid tabulations found three contracts that called for hydro-demolition to a four-inch depth (item code 68645), followed by placement of new concrete (item code 68618 or 68622): L58-C0000110125B01 in Fairfax County, awarded 22 March 2017; N39-C0000110922N01 in the city of Bristol, awarded 28 March 2018; and A34-C0000095861B11B in Buckingham County, awarded 20 March 2019. The size of the jobs, in terms of the hydro-demolition, ranged from 341 to 930 square yards. Among the eight bids on these three contracts, the unit price of hydro-demolition ranged from $90 to $400 per square yard, with a median of (125+157)/2 = $141 per square yard. The unit price of replacement deck concrete (quoted in dollars per cubic yard), when converted to dollars per square yard at a four-inch depth, ranged from $20 to $147.22 per square yard, with a median of (122.22+127.77)/2 = $125 per square yard. As the highest and lowest unit prices for hydro-demolition did not happen to accompany the highest and lowest unit prices for concrete replacement, the unit price of the two activities combined ranged from $110 to $472.22 per square yard, with a median of (265.55+272.22)/2 = $268.88 per square yard.

Historical Estimate of the Unit Cost of Milling and Replacement

A search of the recent VDOT bid tabulations found seven contracts that called for milling to a one-and-a-half-inch depth (item code 68315), followed by placement of new concrete (item code 68605, 68621, or 68910): J13-C000090185B11 in Roanoke County, awarded 24 February 2016; J12-C000084471 in Botetourt County, awarded 24 February 2016; L18-C0000105538B15 in Franklin County, awarded 22 February 2017; L38-C0000108176B53 in Albemarle County, awarded 25 January 2017; N38-C0000111925N01 in the city of Staunton, awarded 28 March 2018; A42-C0000110578B79 in Washington County, awarded 19 December 2018; and A40-C0000114301B77 in Botetourt County, awarded 23 January 2019. The size of the jobs, in terms of the milling, ranged from 575 to 8,742 square yards. Among the nineteen bids on these seven contracts, the unit price of milling ranged from $15.35 to $175 per square yard, with a median of $29.10 per square yard. The unit price of replacement deck concrete (quoted in dollars per cubic yard for codes 68605 and 68621, in dollars per square yard for code 68910), when converted to dollars per square yard at a one-and-a-half-inch depth, ranged from $38.83 to $220 per square yard, with a median of $72.92 per square yard. As the highest and lowest unit prices for milling did not happen to accompany the highest and lowest unit prices for concrete replacement, the unit price of the two activities combined ranged from $59.15 to $252.04 per square yard, with a median of $160.45 per square yard.

Only a single contract, L58-C0000110125B01 in Fairfax County, awarded 22 March 2017, called for milling to 1¾ inches' depth (item code 68316).

The Cost of Incorrectly Estimating Deck Damage

The estimates from the bid tabulations show, unsurprisingly, that hydro-demolition and replacement of four inches of concrete cost over $100 more per square yard of deck than do milling and replacement of one-and-a-half inches of concrete. The cost penalty that the agency will incur if they misidentify deep damage as shallow damage – a "false negative" – will be the cost of the ineffective treatment: in this case, about $160.45 per square yard if they contract for milling and replacement to 1½ inches' depth when hydro-demolition and replacement to 4 inches' depth were needed. The cost penalty that the agency will incur if they misidentify shallow damage as deep damage – a "false positive" – will be the amount by which the cost of the selected treatment exceeds the cost of the needed treatment: in this case, about $108.43 per square yard if they contract for hydro-demolition and replacement to 4 inches' depth when milling and replacement to 1½ inches' depth would have sufficed.

If the incorporation of TLIRT into the condition assessment protocol for bridge decks enables VDOT to identify the extent of shallow and deep delaminations more precisely, it is possible by the above logic to attribute a dollar value to the degree of improvement. Each 1% reduction in the probability of a "false negative" – that is, in the probability of prescribing treatment for a 1½-inch-deep delamination when the actual delamination is deeper – will bring an expected cost saving of $1.6045 per square yard. Each 1% reduction in the probability of a "false positive" – that is, in the probability of prescribing treatment for a deep delamination when treatment for a 1½-inch-deep delamination is all that is required – will bring an expected cost saving of $1.0843 per square yard.

ACKNOWLEDGMENTS

This work was performed under contract to the Virginia Department of Transportation (VDOT). The authors would like to acknowledge the funding and professional input by both VDOT and the Virginia Transportation Research Council (VTRC). Additionally, it should be noted that the physics-based UHC program is the focus of a Ph.D. dissertation. Once published, a copy of the dissertation, authored by Chad M. Anderson, which will include experimental validation, may be obtained from the University of Virginia.

REFERENCES

ASTM D4788-03(2013), *Standard Test Method for Detecting Delaminations in Bridge Decks Using Infrared Thermography*, ASTM International, West Conshohocken, PA, 2013, www.astm.org

Chadbourn, Bruce A., Luoma, James A., Newcomb, David E., Voller, Vaughan R., Consideration of Hot-Mix Asphalt Thermal Properties During Compaction*, ASTM Special Technical Publication 1299*, ASTM International, West Conshohocken, PA, 1996, pp. 127-141 www.astm.org

Cengel, Yunus A. and Afshin J. Ghajar. *Heat and Mass Transfer: Fundamentals & Applications.* 4th ed., ISBN: 978-0-07-339812-9, McGraw-Hill: New York, 2011.

Gilroy, N. *Global Horizontal Solar Resource of Virginia*, April 4, 2017. https://www.nrel.gov/gis/solar.html Accessed May 24, 2019.

Washer GA, Dawson J, Ruiz-Fabian P, Sultan A, Trial M, Fuchs P, et al. Field testing of hand-held infrared thermography, phase II TPF-5(247): final report. 2016.

APPENDIX

DETERMINATION OF THE AVERAGE CONVECTIVE HEAT TRANSFER COEFFICIENTS

Based on text book heat transfer equations, the following calculations were performed (Cengel 2011). In the case where wind velocity is trivial and convective heat transfer is governed by natural buoyancy (natural convection control), a conservative average value was determined in the following way, using the relationship shown in Equation 7. This equation relates the average natural convection Nusselt number (Nu), to the convective heat transfer coefficient. However, prior to the calculation of the Nusselt number, the Rayleigh number (Ra), shown by Equation 8, needed to be determined.

$$Nu = \frac{h_{conv} L_c}{\kappa_{air}} \qquad \text{Equation 7}$$

$$R_a = \frac{g\beta(\ _s - \ _\infty){L_c}^3}{\nu} Pr \qquad \text{Equation 8}$$

To determine the Rayleigh number, a representative slab size was first selected. For the parametric study a 12 [ft.] by 12 [ft.] (approximately 3.66 [m] by 3.66 [m]) flat horizontal slab was used. This permits the calculation of the characteristic length (L_c). As shown by Equation 9, for a horizontal plate, the characteristic length is defined as the convective surface area (A_s) divided by the plate's perimeter(p).

$$L_c = \frac{A_s}{p} = \frac{3.66\ [m] \times 3.66[m]}{4 \times 3.66\ [m]} = 0.915[m] \qquad \text{Equation 9}$$

Next the air film temperature (T_f) was calculated using Equation 10, so that the coefficient of volume expansion(β) could be calculated by Equation 11.

$$T_f = \frac{(\ _s + \ _\infty)}{2} = \frac{(35[℃] + 23.9[℃])}{2} = 29.5[℃] \qquad \text{Equation 10}$$

$$\beta = \frac{1}{_f[K]} = \frac{1}{29.5 + 273} = \frac{1}{302.5[K]} \qquad \text{Equation 11}$$

To calculate the air film temperature, reasonable ambient (T_∞) and deck surface (T_s) temperatures were selected. Based on the air film temperature, the kinematic viscosity(ν), Prandtl number (Pr) and thermal conductivity of the air (κ_{air}) was selected from air property tables. These values along with the gravitational constant (g) were used to determine the Rayleigh number, shown by Equation 12.

$$R_a = \frac{9.81\ \left[\frac{m}{s^2}\right] \times \left(\frac{1}{302.5[K]}\right) \times (35 - 23.9[K]) \times (0.915[m])^3}{\left(1.603 \times 10^{-5}\ \left[\frac{m^2}{s}\right]\right)^2} 0.7284 = \ 7.81 \times 10^8$$

Equation 12

Based on the calculated Rayleigh number, the Equation 13 and 14 were used to determine the Nusselt numbers for the top and bottom surface of the deck, respectively.

$$Nu_{\ op} = 0.15{R_a}^{1/3} = 0.15 \times (7.81 \times 10^8)^{\frac{1}{3}} = 138 \qquad \text{Equation 13}$$

$$Nu_{Bot} = 0.27{R_a}^{1/4} = 0.27 \times (7.81 \times 10^8)^{\frac{1}{4}} = 45 \qquad \text{Equation 14}$$

Using Equation 7, the convective heat transfer coefficients for the top and bottom of the slab, were estimated to be as shown (equation 15 and 16, respectively).

$$h_{conv\_\ op} = \frac{Nu_{\ op}}{L_c}\,\kappa_{air} = \frac{138}{0.915[m]} \times 0.02584\ [W/m\,K] = 3.90[W/m^2\,K]$$

Equation 15

$$h_{conv\_Bot} = \frac{Nu_{Bot}}{L_c}\,\kappa_{air} = \frac{45}{0.915[m]} \times 0.02584\ [W/m\,K] = 1.27[W/m^2\,K]$$

Equation 16

In the case where wind velocity is not trivial and convective heat transfer is governed by the wind currents (forced convection control), a conservative average heat transfer coefficient value was determined using equations governing forced external convection. It was calculated that the average convective heat transfer coefficients for the deck (top and bottom) exposed to a wind velocity of 10 [mi/h] (16 [km/h]) would result in a value of approximately 21 [W/m^2 K].